# How Intracranial Thrombi Embed Along The Stent Retriever Following Mechanical Thrombectomy. A High-Resolution Scanning Electron Microscopy Analysis.

**Daniela Dumitriu La Grange** ( Daniela.DumitriuLagrange@unige.ch )
University of Geneva
**Gianmarco Bernava**
University of Geneva
**Philippe Reymond**
University of Geneva
**Isabel Wanke**
Klinik Hirslanden Zurich
**Maria Isabel Vargas**
University of Geneva
**Paolo Machi**
University of Geneva
**Karl-Olof Lövblad**
University of Geneva

**Research Article**

**Keywords:** Endovascular, stent, thrombectomy, compact

**Posted Date:** November 2nd, 2021

**DOI:** https://doi.org/10.21203/rs.3.rs-951665/v1

# Abstract

Endovascular treatment with stent retriever thrombectomy is a major advancement in the standard of care in acute ischemic stroke (AIS). The modalities through which thrombi embed along stent retriever following mechanical thrombectomy (MTB) remain to be elucidated. Using scanning electron microscopy (SEM), we analyzed the behavior of thrombi embedded onto the stent, when retrieved by MTB from patients, victims of AIS. We observed that incorporation of thrombi is achieved through loosely packed, non-compact regions. We hypothesize that structural heterogeneity modulation of thrombi, in terms of compact and non-compact regions, is related to the endovascular treatment outcome.


# 1. Introduction

Endovascular treatment using stent retriever (SR) thrombectomy revolutionized the standard of care in acute ischemic stroke (AIS),[1 2 3 4 5 6 7 8 9] which is the first cause of acquired deficit and second cause of death in the occidental world. The modalities through which thrombi attach to stent retriever struts are still to be elucidated. Knowledge about the deformability and friction properties of main components of thrombi, red blood cells,[10] and fibrin,[11 12] enables scientists to design parametric studies in vascular phantoms and to anticipate the effectiveness of various thrombectomy techniques,[13 14]. Nevertheless, compared to thrombi artificially generated in vitro, thrombi retrieved from patients are inherently more complex and diverse in terms of composition and morphology, [15]. A recent study focused on mechanical properties of human stroke thrombi retrieved with endovascular techniques reports that fibrin/platelet content is associated with increased thrombus stiffness, and red blood cells content with decreased stiffness, [16]. Because human thrombi differ from the thrombi generated in vitro in terms of structural organization, they also differ in stiffness, [16]. As today, the microscopical features that favor the human thrombi incorporation into the stent are not yet explored. Among the ex vivo characterization techniques, scanning electron microscopy (SEM) can render morphological information about the thrombus cellular content and fibrin organization,[17 18] and is the only technique capable of providing with high resolution relevant details for the interface between thrombus and stent. In this respect, the ex vivo studies conducted so far on stent-thrombus attachment are scarce, and, while pointing out mechanical entrapment and adhesion,[19 20] as main means of thrombus incorporation, they are limited to the outer view of thrombi.

In this study, we analyzed with microscopy images the modalities in which two compositionally different thrombi retrieved from patients are incorporated into the stent retriever, and we highlighted their underlying structural characteristics and their commonalities in anchoring on to the stent.

# 2. Methods

The followed procedures were in accordance with the ethical standards of the responsible committee on human experimentation (institutional and national) and with the *Helsinki Declaration* of 1975, as revised

in 2008. The study was approved, under the project ID 2018-00476, by the Cantonal Commission of Research Ethics (Commission cantonale d'éthique de la recherche, CCER) Geneva, who waived the requirement for informed consent, under the Art.34 LRH, Art.37-40 ORH.

### 2.1. Endovascular technique:

The thrombi were retrieved from patients suspected of being victims of acute ischemic stroke (AIS), received whole brain stroke CT protocol [5] and were referred for MTB intervention. Thrombectomy procedures were performed under general anesthesia using a bi-plane C-arm (Allura Clarity FD20, Philips Healthcare, Best, the Netherlands) via a common femoral artery approach. A guiding catheter was placed in the concerned artery at neck level. A large-bore aspiration-catheter was advanced over a microcatheter and a microwire up to the thrombus, while the microcatheter was advanced beyond the thrombus.

Subsequently, a stent retriever (Catch-Mini3, Balt, Montmorency, France; TREVO Striker, Kalamazoo, Michigan, USA) was advanced through the microcatheter and unsheathed across the thrombus. Hence, the SR was gently retrieved inside the large bore aspiration catheter while a negative pressure was applied through it by using a vacuum system.

### 2.2. Sample preparation and microscopy technique:

Upon retrieval, thrombi integrated onto the stent were first immersed in formalin (4%), and immediately after were transferred in glutaraldehyde (2.5%), where they were kept overnight at 4 °C. Subsequently, samples were washed in phosphate buffer solution (PBS) 10X three times for 20 minutes each, dehydrated in solutions of ascending concentrations of ethanol (50, 60, 70, 80, 90, 100%) for 15 minutes each time, and dried using critical point drying. The samples were mounted on SEM stubs using carbon tape and carbon paint and sputtered with a 5 nm AuPd (80%/20%) coating. The microscopy observations were performed with an ultra-high-resolution field-emission Zeiss Merlin SEM, equipped with a Gemini II column, using the Everhart-Thornley secondary electron detector, 5 kV acceleration voltage and 500 pA probe current.

We illustrate our analysis with two thrombi retrieved by MTB, after a single SR pass, from two patients victims of AIS. In both cases, the thrombus was located within the M2 segment of the middle cerebral artery (MCA). In the first case (Case 1), the stent used was a Catch-Mini3, while in the second case (Case 2), the stent was a Trevo. The volume of retrieved thrombus was approximately 2 $mm^3$ in Case 1 and 50 $mm^3$ in Case 2.

## 3. Results

The microscopy observations showed that the two thrombi differ in terms of composition and structure. In addition, each thrombus showed intrinsic heterogeneity.

### 3.1. Results - Microscopy examination for Case 1:

Figure 1 presents the optical (Figure 1a) and the electron microscopy (Figure 1b) views of the thrombus attached to the stent retriever. The thrombus is integrated in the stent by being wrapped around one of the stent struts and has a compact appearance. Higher magnification view (Figure 1c) of the stent-thrombus interface is showing non-adhesion and a dense fibrin rich outer surface.

Figure 2a depicts fragments of the same thrombus after being sectioned along perpendicular directions. The bigger section reveals folding of a thick (100-200 micrometers), dense fibrin sheet, with fibrin fibers clearly visible in higher magnification micrographs. A fracture, visible on one of the faces, indicates fibrin fibers organization in bundles with a preferred parallel orientation to each other and perpendicular relative to the stent direction (Figure 2a and b). White cells are incorporated into the dense fibrin sheet, with an estimate density of 2-to-4 cells per 1000 $\mu m^3$, or roughly 15% of the volume, while the fibrin fibers occupy, in this dense part of the thrombus, an estimated 70-80% of the local volume. The folding of fibrin sheets forms a cavity, which was inconspicuous prior to sectioning. Infrequent clusters of biconcave red blood cells and white blood cells are scattered through the cavity (Figure 2c). A closer view within the cavity and examination of the inner walls shows that fibrin fibers aggregate in large bundles, which, although cross linked in a fine weave, are aligned, at larger scale, in parallel to each other (Figure 2d). A closer view of the smaller thrombus fragments (marked “3” in Figure 2a), originally wrapped around the stent strut, is showing a loosely packed fibrin network with no cellular content (Figure 2e) interweaved with more compact aggregates, which consist of polyhedral red blood cells and white cells encased in fibrin mesh (Figure 2f). The estimated cellular content, based on microscopy images, is 10-20% of the local volume. However, the porosity of fibrin is increased several folds in the region of thrombus wrapped around the stent strut, compared with the bulk part, away from stent.

### 3.2. Results - Microscopy examination for Case 2:

The optical view and a collage of scanning electron micrographs of the thrombus retrieved in Case 2, integrated in the stent, are shown in Figure 3. The integrated thrombus spirals along the stent, with multiple attachment points, with its various segments being anchored on single or two stent struts at a time.

Closer views of selected attachment points representative for thrombus anchoring modes are presented in Figures 3 and 4. The inner content of thrombus consists in red blood cells, while the outer layer is formed by fibrin. This finding is consistent with previous description of cerebral arterial thrombi,[21 22]. The thrombus compactness is variable, from its peripheral regions towards the core, and along its length.

Figure 3c-f presents the segment closest to the stent tip (marked with dashed yellow in Figure 3b). The low magnification view (Figure 3c) shows that thrombus is anchored as such that allows a large contact area with the stent strut, and physically incorporates the stent. A closer view in Figure 3d shows the stent protruding from the thrombus, which at this location is formed by loosely packed red blood cells and a thin, well segregated from the red blood cells volume region, outer layer of fibrin. As Figure 3e is indicating, the fibrin at this site incorporates a large number of platelets and white cells. A cross section

of the bulky segment of thrombus, which is illustrative for thrombus overall composition, is shown in Figure 3f. While the outer surface is formed by fibrin fibers, the cross section indicates a periphery where the red blood cells are the main component and intercalate fibrin, and a gradual increase in compactness towards a core of polyhedral red blood cells. The polyhedral shape of red blood cells is acquired due to compressive forces in vivo, and is a marker for intravital thrombus contraction,[23 24 25].

The stent protruding through the thrombus matter is visible at several anchoring points, and always at sites of loose cellular packing, as indicated by the biconcave shape of the red blood cells. Figure 4a and b depicts a cap-like accumulation of platelets at the site where the stent is protruding. As observed in Figure 4b, the large number of platelets is adjacent to biconcave red blood cells, while the intercellular fibrin content is scarce. Another modality of anchoring is illustrated in Figure 4, c and d. In this case, at the contact point with the stent, the thrombus is conforming with the stent strut shape, which indicates amenability for deformation and affinity for the stent surface. Higher magnification view of the contact area is showing flattened red blood cells encased in a fibrin network, along with scattered platelets. Figure 4e is illustrating another protruding site, a thin part of thrombus (10-30 micrometers) of loosely packed biconcave red blood cells covered in an outer layer of fibrin.

In the particular case of this thrombus, we observed that between the double struts of the stent mesh there are films, or bridges, of fibrin, with or without cellular content. Examples are shown in Figure 4c and Figure 4f. It can be argued that such fibrin bridges are not native to the original thrombus that caused the stroke, but instead are formed during the retrieval process. It can be hypothesized that the formation of fibrin bridges aids in the retrieval process.

# 4. Discussion

### 4.1. Discussion - Structural interpretation of microscopy results in Case 1:

Based on the analysis of SEM images, we reconstruct the thrombus architecture in Case 1 as following. The fibrin is the main, and ubiquitous structural element in this case, while red blood cells content is scarce and non-uniformly distributed. The thrombus incorporation into the stent is non-adhesive and relies on foldability, or in other words on the ability of thrombus matter to wrap itself around the stent strut. At the whole thrombus scale, we can define, qualitatively but relevant, two types of aggregates.

In type I, fibrin is organized in textured, compact and fairly uniform large aggregates having a high aspect ratio (sheet like, 100-200 microns thick, several hundreds of microns wide), in which fibrin bundles function as structural reinforcement elements. In the apparent direction of the fibrin bundles, the bending angle of thrombus sheet is large and indicates resistance to deformation. Bending at smaller angles and torsional deformation occur in other directions.

In type II, micro-regions of fibrin with embedded cellular content (red blood cells, and other cellular content) are intercalated between micro-regions of highly porous, non-compact fibrin with no cellular content, rendering a short-range (within tens of micrometers) structural heterogeneity. Apparently, in

contrast to type I, in type II aggregate the randomly oriented micro-regions with variable compactness allow flexibility and multidirectional deformation. In conclusion, for the fibrin rich thrombus analyzed in Case 1, the increased porosity and short-range heterogeneity are responsible for thrombus fitting around the stent strut.

### 4.2. Discussion - Structural interpretation of microscopy results in Case 2:

After examining the thrombus retrieved in Case 2, we can conclude the following. The thrombus incorporates multiple segments of bulky, compact aggregates of red blood cells, in which fibrin is peripheral. Platelets are scattered on the outer layer of fibrin or form a cap-like aggregate at one of thrombus segments. The compact aggregates show neither adherence to the stent strut, nor foldability, and they are the segments of the thrombus that evade anchoring on the stent. However, the compact aggregates are linked through loosely packed volume regions of red blood cells. The non-compact volume regions show deformability, wetting properties for the stent surface, and often allow the stent struts to protrude. The thrombus displays a long range (millimeters) heterogeneity in compactness. As such, for the red blood cells rich thrombus in Case 2, densely packed regions, formed of polyhedrocites, render mechanical resistance and alternate with loosely packed regions, which provide the opportunity for anchoring to the stent struts.

Our analysis of thrombi retrieved by MTB with SR highlights the idea that the intra-thrombus heterogeneity in structural density, or variation in compactness, accompanies the thrombus attachment onto the stent. Previously it was shown that the intravital contraction, or compactness, of red blood cells rich thrombi makes them less susceptible to external fibrinolysis,[26]. In addition, it was suggested [16] that thrombus intra-vital contraction is a contributor to stiffness. Our study suggests that thrombi compact regions, whether they are formed by polyhedrocites or compact fibrin, are not susceptible to attaching on to the stent, while the amenability of non-compact regions to deform favors thrombus incorporation into the stent. Therefore, it is safe to assume that the extent of compact regions in thrombus can affect its incorporation into the stent and influence the outcome of MTB. It is recognized that thrombi undergo structural changes, during and after retrieval process by MTB, [27]. Standard procedures are needed, indeed, as such that the results of structural analysis of thrombi retrieved by MTB can be correlated with the structural organization of thrombi at the arterial occlusion site, in patients victims of AIS.

A detailed examination of human thrombi when attached to stent retrievers can offer new insights on the efficacy of thrombectomy devices and can help, with the aid of clinical neuroimaging, make better choices of stent retriever design, as such that the efficacy of MTB can be improved. So far, and with the purpose of recognizing clinical neuroimaging signs predictive for the treatment outcome,[28 29] an empirical dichotomous categorization was established for the underlying histopathology of thrombi. According to this categorization, thrombi with a fairly rich content in erythrocytes are amenable to mechanical thrombectomy (MTB),[30 31] and fibrin rich thrombi are resilient to endovascular techniques,[31]. However, for enabling personalized treatment, there is a need to establish more accurate approaches which link clinical neuroimaging with the biomechanical factors governing thrombi

incorporation into the stent retriever,[5] and nevertheless with their structural organization. Microstructural examination of human thrombi can help fill the existing knowledge gaps.

# 5. Conclusions

The successful incorporation of thrombi along the stent retrievers is achieved through anchoring at sites that are non-compact and deformable, either by wrapping around the stent struts, by conforming with (wetting) the stent surface or by allowing the stent struts to protrude. Compact regions, whether fibrin or polyhedrocites, are not susceptible to be anchoring sites. We hypothesize that the extent of compact and non-compact regions in intracranial thrombus is related to the endovascular treatment outcome.

# Declarations


### Acknowledgements:

This work was supported by Swiss National Science Foundation, projects 320030_188942 and 32003B_182382. We thank Dr. Graham Knott for providing the SEM sample preparation protocol, and we thank to Marie Croisier, from Biological Electron Microscopy Facility (BioEM), Ecole Polytechnique Fédérale de Lausanne (EPFL) for critical point drying. The Zeiss Merlin SEM used by the corresponding author for microscopy observations is part of Interdisciplinary Center for Electron Microscopy (CIME), EPFL.


### Author contributions:

D.D.L. designed the experiments and performed the SEM observations, prepared the figures and wrote the main manuscript text. G.B. performed the thrombectomy. G.B., P.R. and P.M. validated the methodology and the results. P.M. and K.O.L. acquired funding. All authors reviewed and edited the manuscript.

### Additional information:

The authors declare that they have no known competing financial interests or personal relationships that could have appeared to influence the work reported in this paper.

The data that support the findings of this study are available on request from the corresponding author.

# References


1. Bernava, G. *et al.* Direct thromboaspiration efficacy for mechanical thrombectomy is related to the angle of interaction between the aspiration catheter and the clot. *J. NeuroInterventional Surg.* **12**, 396–400 (2020).

2. Bernava, G. *et al.* Experimental evaluation of direct thromboaspiration efficacy according to the angle of interaction between the aspiration catheter and the clot. *J. NeuroInterventional Surg.* neurintsurg-2020-

016889 (2021) doi:10.1136/neurintsurg-2020-016889.

3. Campbell, B. C. V. *et al.* Safety and Efficacy of Solitaire Stent Thrombectomy: Individual Patient Data Meta-Analysis of Randomized Trials. *Stroke* **47**, 798–806 (2016).

4. Hofmeister, J. *et al.* The Catch Mini stent retriever for mechanical thrombectomy in distal intracranial occlusions. *J. Neuroradiol. J. Neuroradiol.* **45**, 305–309 (2018).

5. Hofmeister, J. *et al.* Clot-Based Radiomics Predict a Mechanical Thrombectomy Strategy for Successful Recanalization in Acute Ischemic Stroke. *Stroke* **51**, 2488–2494 (2020).

6. Machi, P., Luft, A., Winklhofer, S., Anagnostakou, V. & Kulcsár, Z. Endovascular treatment of acute ischemic stroke. *J. Neurosurg. Sci.* (2020) doi:10.23736/S0390-5616.20.05109-7.

7. Machi, P. *et al.* Solitaire FR thrombectomy system: immediate results in 56 consecutive acute ischemic stroke patients. *J. Neurointerventional Surg.* **10**, i27–i32 (2018).

8. Maus, V. *et al.* Intracranial mechanical thrombectomy of large vessel occlusions in the posterior circulation using SAVE. *BMC Neurol.* **19**, 197 (2019).

9. Mokin, M. *et al.* Indications for thrombectomy in acute ischemic stroke from emergent large vessel occlusion (ELVO): report of the SNIS Standards and Guidelines Committee. *J. NeuroInterventional Surg.* **11**, 215–220 (2019).

10. Kim, Y., Kim, K. & Park, Y. Measurement Techniques for Red Blood Cell Deformability: Recent Advances. in *Blood Cell - An Overview of Studies in Hematology* (ed. Moschandreou, T.) (InTech, 2012). doi:10.5772/50698.

11. Gunning, G. M. *et al.* Clot friction variation with fibrin content; implications for resistance to thrombectomy. *J. NeuroInterventional Surg.* **10**, 34–38 (2018).

12. Litvinov, R. I. & Weisel, J. W. Fibrin mechanical properties and their structural origins. *Matrix Biol.* **60–61**, 110–123 (2017).

13. Madjidyar, J., Pineda Vidal, L., Larsen, N. & Jansen, O. Influence of Thrombus Composition on Thrombectomy: ADAPT vs. Balloon Guide Catheter and Stent Retriever in a Flow Model. *RöFo - Fortschritte Auf Dem Geb. Röntgenstrahlen Bildgeb. Verfahr.* **192**, 257–263 (2020).

14. Sanchez, S. *et al.* ANCD thrombectomy device: in vitro evaluation. *J. NeuroInterventional Surg.* **12**, 77–81 (2020).

15. Staessens, S. *et al.* Structural analysis of ischemic stroke thrombi: histological indications for therapy resistance. *Haematologica* **105**, 498–507 (2020).

16. Boodt, N. *et al.* Mechanical Characterization of Thrombi Retrieved With Endovascular Thrombectomy in Patients With Acute Ischemic Stroke. *Stroke* **52**, 2510–2517 (2021).

17. Chernysh, I. N. *et al.* The distinctive structure and composition of arterial and venous thrombi and pulmonary emboli. *Sci. Rep.* **10**, 5112 (2020).

18. Tomaiuolo, M., Litvinov, R. I., Weisel, J. W. & Stalker, T. J. Use of electron microscopy to study platelets and thrombi. *Platelets* **31**, 580–588 (2020).

19. Autar, A. S. A. *et al.* High-Resolution Imaging of Interaction Between Thrombus and Stent-Retriever in Patients With Acute Ischemic Stroke. *J. Am. Heart Assoc.* **7**, (2018).

20. van Es, A. C. G. M. *et al.* Imaging stent–thrombus interaction in mechanical thrombectomy. *Neurology* **88**, 216–217 (2017).

21. Ahn, S. H. *et al.* Histologic features of acute thrombi retrieved from stroke patients during mechanical reperfusion therapy. *Int. J. Stroke* **11**, 1036–1044 (2016).

22. Weisel, J. W. & Litvinov, R. I. Visualizing thrombosis to improve thrombus resolution. *Res. Pract. Thromb. Haemost.* rth2.12469 (2021) doi:10.1002/rth2.12469.

23. Cines, D. B. *et al.* Clot contraction: compression of erythrocytes into tightly packed polyhedra and redistribution of platelets and fibrin. *Blood* **123**, 1596–1603 (2014).

24. Peshkova, A. *et al.* Reduced Contraction of Blood Clots in Venous Thromboembolism Is a Potential Thrombogenic and Embologenic Mechanism. *TH Open* **02**, e104–e115 (2018).

25. Tutwiler, V. *et al.* Shape changes of erythrocytes during blood clot contraction and the structure of polyhedrocytes. *Sci. Rep.* **8**, 17907 (2018).

26. Tutwiler, V. *et al.* Blood clot contraction differentially modulates internal and external fibrinolysis. *J. Thromb. Haemost.* **17**, 361–370 (2019).

27. Xu, R.-G. & Ariëns, R. A. S. Insights into the composition of stroke thrombi: heterogeneity and distinct clot areas impact treatment. *Haematologica* **105**, 257–259 (2020).

28. Duffy, S. *et al.* Per-Pass Analysis of Thrombus Composition in Patients With Acute Ischemic Stroke Undergoing Mechanical Thrombectomy. *Stroke* **50**, 1156–1163 (2019).

29. Ye, G. *et al.* Association Between Thrombus Density and Reperfusion Outcomes Using Different Thrombectomy Strategies: A Single-Center Study and Meta-Analysis. *Front. Neurol.* **10**, 843 (2019).

30. Maekawa, K. *et al.* Erythrocyte-Rich Thrombus Is Associated with Reduced Number of Maneuvers and Procedure Time in Patients with Acute Ischemic Stroke Undergoing Mechanical Thrombectomy. *Cerebrovasc. Dis. Extra* **8**, 39–49 (2018).

31. Moftakhar, P. *et al.* Density of Thrombus on Admission CT Predicts Revascularization Efficacy in Large Vessel Occlusion Acute Ischemic Stroke. *Stroke* **44**, 243–245 (2013).

# Figures

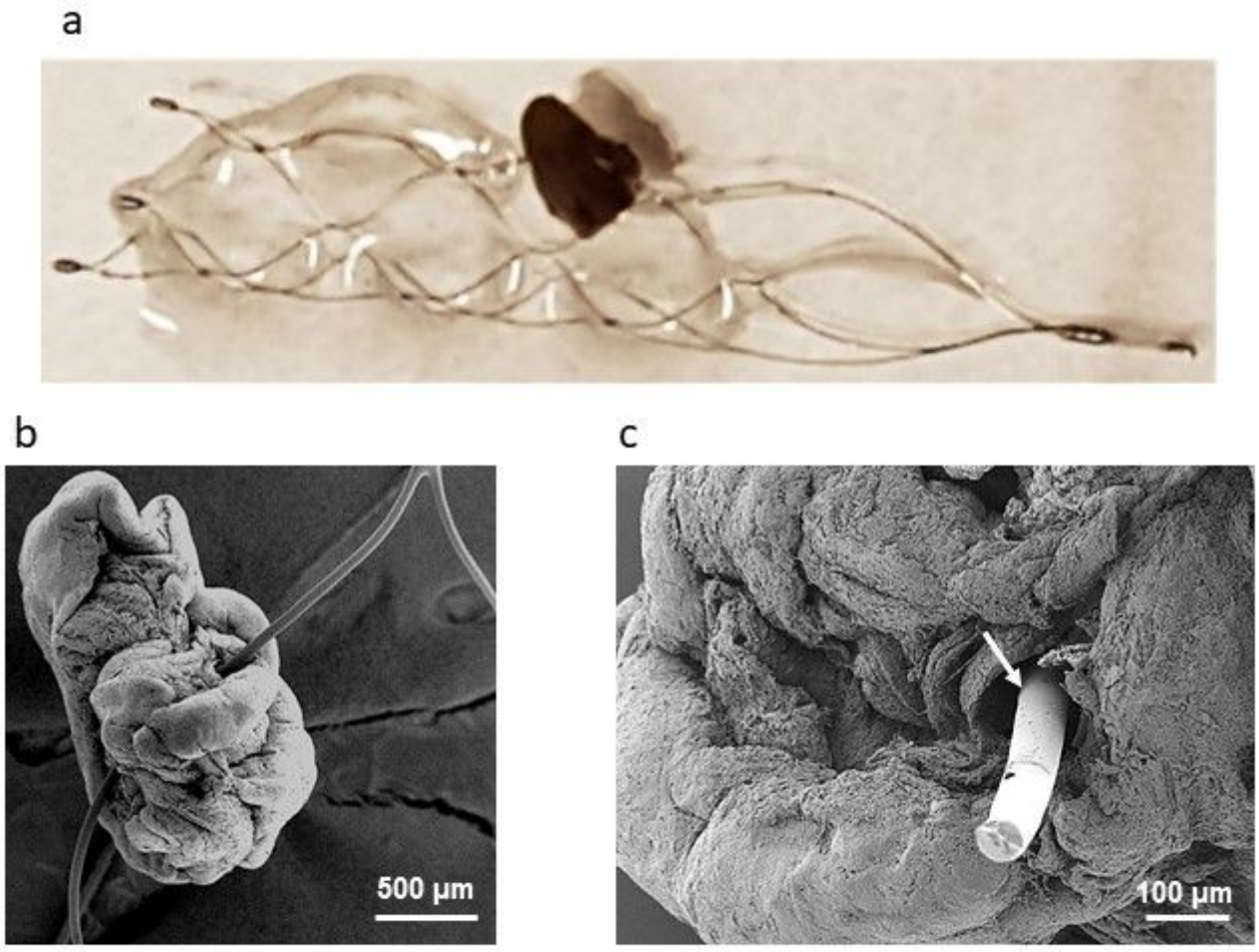


**Figure 1**

Thrombus retrieved in Case 1 integrated in the stent retriever. a. Optical micrograph (thrombus fixed in formalin). b. Low magnification SEM view of the same thrombus (anchored on the stent strut). c. Closer SEM view at the thrombus-stent interface (the stent strut was cut, to allow better viewing). There is no adhesion between the thrombus and the stent strut (arrow).

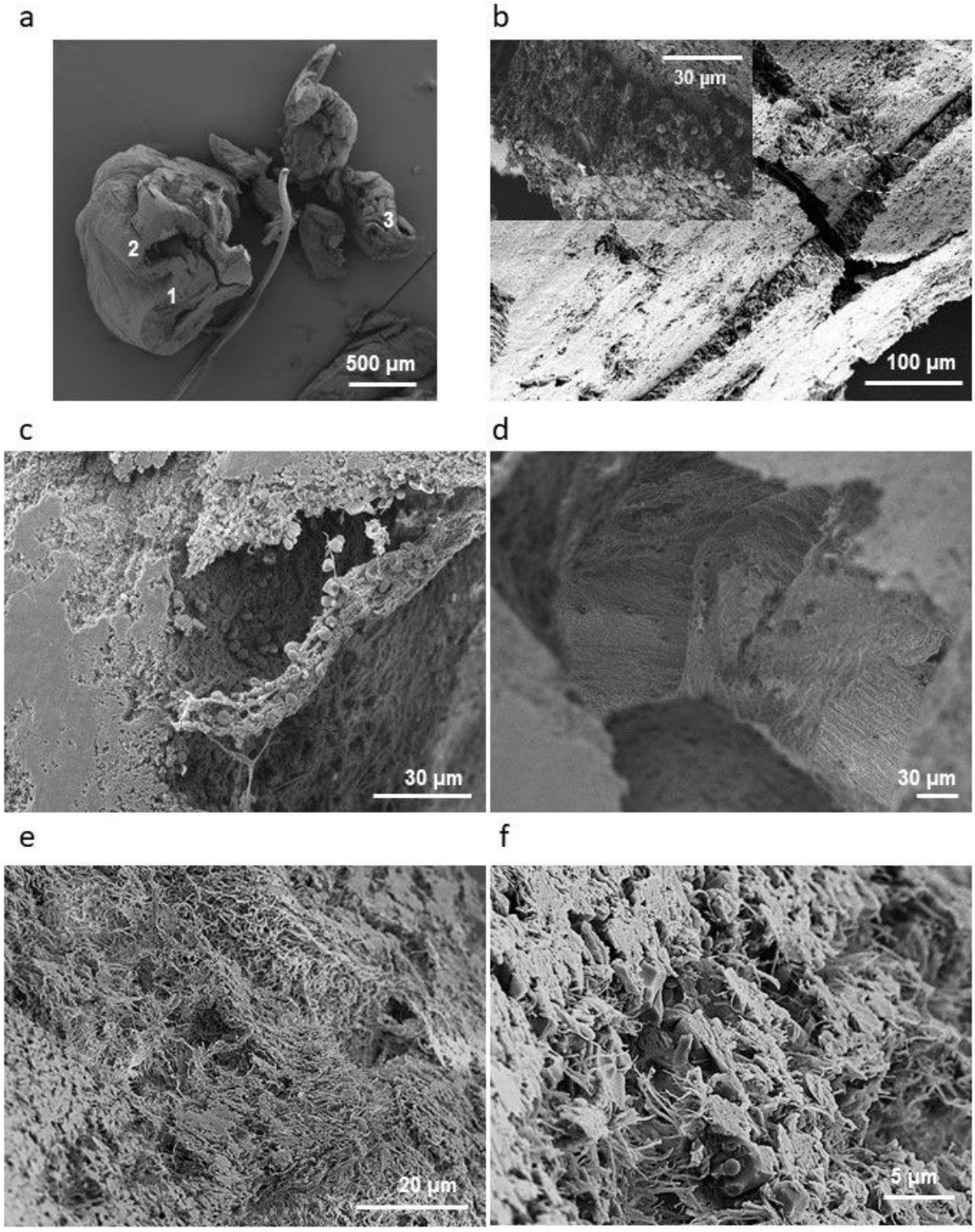


## Figure 2

Analysis of thrombus retrieved in Case 1. a. Cross section of the thrombus retrieved in Case 1. b. Closer view of fracture visible on the bigger section of thrombus (marked with “1” in Figure 2a), and in inset higher magnification of the area marked by the dashed oval. c and d – closer view of the region marked with “2” in Figure 2a. c. Cross section into the wall and scattered red blood cells and white cells inside the cavity. d. Broad view inside the cavity. e, f – cross sections of thrombus segments (marked “3” in Figure

2a) that were wrapped around the stent strut. e. Loosely packed fibrin region. f. Compact region with polyhedral red blood cells, white cells in between the fibrin.

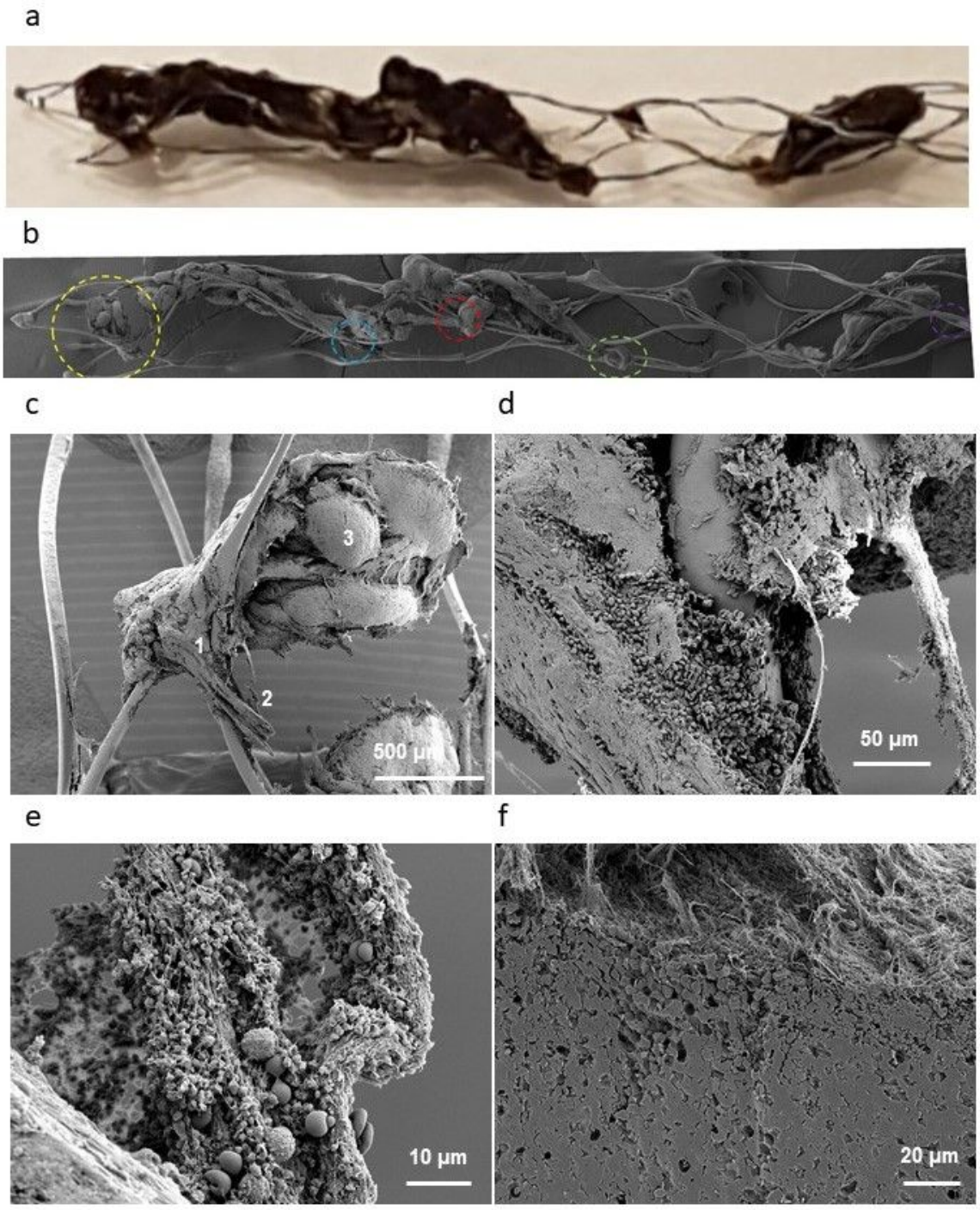


## Figure 3

Thrombus retrieved in Case 2, integrated in the stent retriever. a. Optical micrograph (thrombus fixed in formalin). b. Collage of SEM micrographs depicting the thrombus retrieved in Case 2. c-f: Electron micrographs detailing the structure and composition of the thrombus segment marked in Figure 3 with

yellow dashed circle. c. Overall view of the segment. d. Closer view of the stent-thrombus contact region, marked with “1” in Figure 3c. e. Structure and composition of fibrin bridge, marked with “2” in Figure 3c. f. Cross sectional view after cutting through the bulky region marked with “3” in Figure 3c.

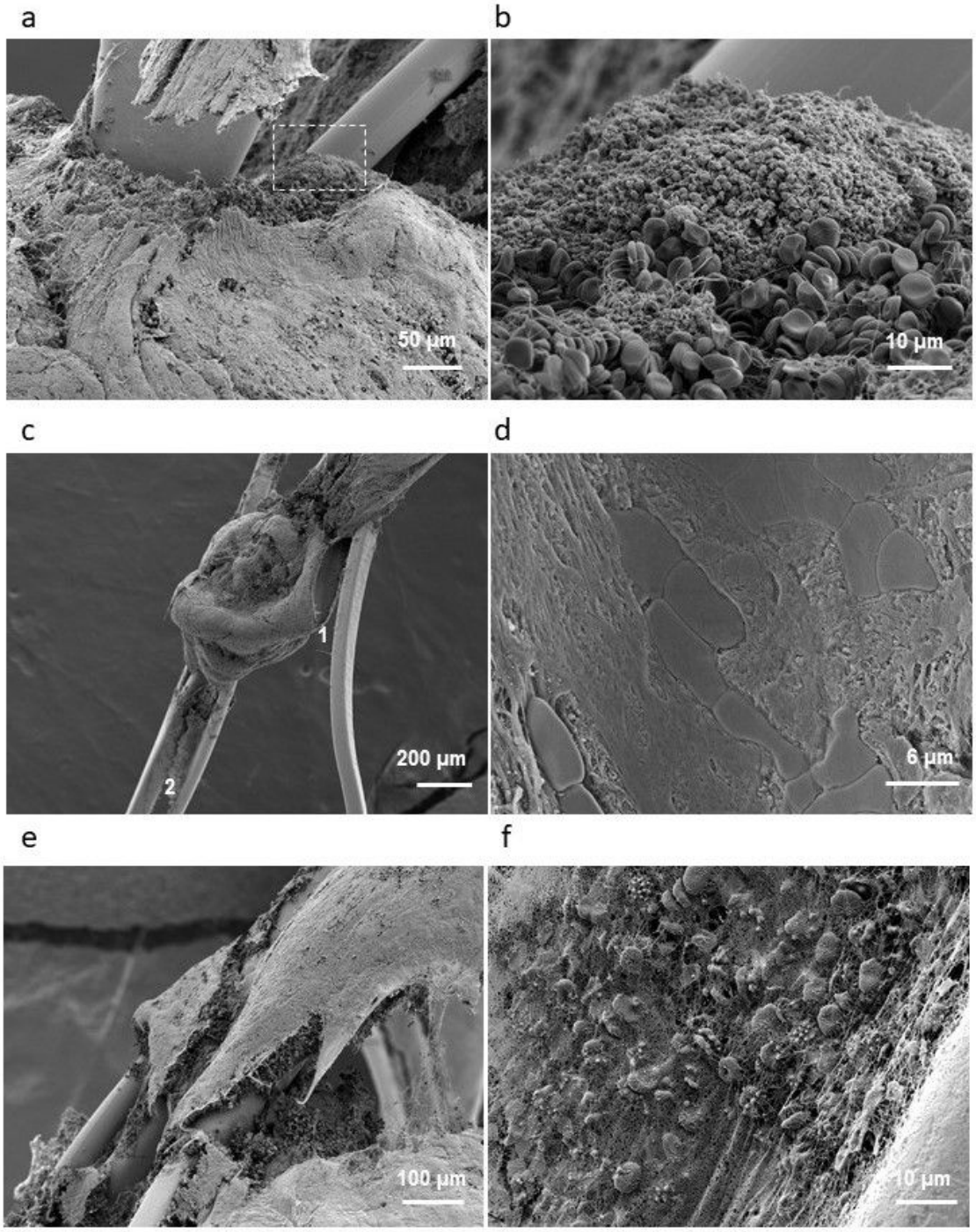


## Figure 4

a. Electron micrograph of the region marked in Figure 3 with red dashed circle, showing one anchoring site with protruding stent strut. b. Close up view of the white insert in Figure 4a, showing platelets

adjacent to red blood cells. c. Close view of the region marked with green dashed circle in Figure 3, showing thrombus conformity with the strut (marked “1”) and a fibrin bridge (marked “2”). d. Inside close up view of the thrombus conforming surface, at the interface with the stent (marked “1” in 3c). e. Close up view of the region marked with blue dashed circle in Figure 3, showing a thin shaped thrombus region of loosely packed red blood cells surrounded by a thin fibrin layer. f. A fibrin film with red and white cells bridging the double stent struts (close up from the region marked with purple dashed circle in Figure 3).